

Revision of the microwave coefficient files in the IFS

Cristina Lupu, Alan J. Geer and Niels
Bormann

Research Department

March 2015

*This paper has not been published and should be regarded as an Internal Report from ECMWF.
Permission to quote from it should be obtained from the ECMWF.*



Series: ECMWF Technical Memoranda

A full list of ECMWF Publications can be found on our web site under:

<http://www.ecmwf.int/en/research/publications>

Contact: library@ecmwf.int

©Copyright 2015

European Centre for Medium-Range Weather Forecasts
Shinfield Park, Reading, RG2 9AX, England

Literary and scientific copyrights belong to ECMWF and are reserved in all countries. This publication is not to be reprinted or translated in whole or in part without the written permission of the Director-General. Appropriate non-commercial use will normally be granted under the condition that reference is made to ECMWF.

The information within this publication is given in good faith and considered to be true, but ECMWF accepts no liability for error, omission and for loss or damage arising from its use.

Abstract

The radiative transfer model RTTOV is an important component of the assimilation of radiance observations and is used in conjunction with a number of regression coefficient files generated for a given instrument and its channels. RTTOV-11 is the latest version and comes with a new set of radiative transfer coefficient files based on 54 fixed vertical pressure levels and the latest underlying spectroscopic parameters. This memorandum summarises the evaluation of RTTOV-11 microwave radiative transfer coefficient files for use in the operational assimilation system at ECMWF. Results show some improvement in the observation fits at first-guess. The change to 54 levels ensures smooth varying layer thicknesses (in particular at the top of the atmosphere) and improves the first-guess fits for ATMS and AMSU-A stratospheric channels. Small changes are noticeable in the mean temperature analyses above 100 hPa. The new specification of the 22 GHz water vapor line width and the inclusion of ozone for channels near 183 GHz for SSMIS, lead to a reduction in the mean bias corrections and reflect better agreement with the observations. The impact of using the newly released set of RTTOV-11 microwave coefficient files on medium-range forecasts is overall neutral. The results presented here suggested that it would be beneficial for the ECMWF operational system to use the most up-to-date version of the microwave coefficient files released with the latest version of RTTOV-11 and this will become operational with IFS cycle 41r2.

1 Introduction

To assimilate radiance measurements from satellites in a numerical weather prediction (NWP) model, a reliable and accurate fast radiative transfer model is required, to establish the relationship between the physical state of the atmosphere and the observable radiation. The Radiative Transfer for the Television Infrared Observation Vertical Sounder model (RTTOV) is continuously maintained and improved by the NWP community and so version 11 (Hocking *et al.*, 2014; Saunders *et al.*, 2013; Matricardi *et al.*, 2004) is the latest developed within the framework of the European Organisation for the Exploitation of Meteorological Satellites NWP-Satellite Application Facility (EUMETSAT NWP-SAF). At the European Centre for Medium-Range Weather Forecasts (ECMWF) efforts are continuously made to ensure that the operational system uses the most up to date version of RTTOV and version 10.2 has been upgraded to version 11.1 in the ECMWF's Integrated Forecasting System (IFS) cycle 40r2. New options for vertical interpolation and Jacobian smoothing (Hocking, 2014) were included in the IFS cycle 40r3. None of these cycles became operational, but the RTTOV-11 upgrade and new interpolation will become operational with cycle 41r1 in May 2015 (Lupu and Geer, 2015). RTTOV-11 supports 41 satellite platforms with a total of 76 different sensors. It comes with a new set of coefficient files specific for a given instrument and its set of infrared (IR) or microwave (MW) channels (Hocking *et al.*, 2014). The newly released coefficient files are based on different atmospheric layering (54 rather than the 44 or 51 levels in previous files) and different or revised spectroscopy.

This study reports on the revision of MW sounder and imager coefficient files used in the ECMWF IFS. At the time of this study the microwave sounders assimilated in the IFS included: the AMSU-A temperature sounders on seven satellites (NOAA-15, -16, -18, -19, MetOp-A, MetOp-B and Aqua), the MHS humidity sounders on four satellites (NOAA-18, -19, MetOp-A and MetOp-B) and the ATMS instrument on S-NPP which combines both temperature and humidity sounding channels (see appendix for meaning of these acronyms). The microwave sounding data from MWTS on FY-3A and MWHS on FY-3A and -3B were passively monitored. The microwave imagers assimilated in the IFS included SSMIS on F-17 and TMI on TRMM. Microwave observations have a significant contribution to temperature (Cardinali, 2009) and impose the dominant constraint on tropospheric humidity over oceans (Geer, 2013;

Geer *et al.*, 2014). Taken collectively as a system, MW observations provide the greatest contribution to forecast accuracy among the range of observation types currently assimilated.

This paper is organized as follows. Section 2 describes the main aspects of the current and the new MW coefficient files used with the RTTOV-11 fast model. Data assimilation experiments were carried out to evaluate the impact of RTTOV-11 MW coefficient files on the ECMWF analyses and forecasts. Section 3 describes the set-up of the experiments, the data used in the experiments and discuss initial analysis and forecast impact of the RTTOV-11 MW coefficient files. Section 4 shows final results from the data assimilation experiments based on the recent ECMWF operational model upgrade (IFS cycle 41r1). The memorandum is concluded by a brief summary and outlook in Section 5.

2 Aspects of the microwave coefficient files used with RTTOV-11

RTTOV is used in conjunction with a number of regression coefficients generated using different line-by-line models and using various profile training sets for different numbers of vertical pressure levels. This section documents the main differences between the newly released and the current set of MW radiative transfer coefficient files.

2.1 Number of fixed pressure levels in the coefficient files

RTTOV computes optical depths on the levels specified in the coefficient files. For the majority of MW instruments used in the IFS the current coefficient files are provided on only 44 fixed vertical pressure levels, where pressure ranges between 1013.25 and 0.05 hPa. Exceptions of coefficient files on 51 fixed vertical pressure levels between 1050.00 and 0.05 hPa include recent sensors, such as ATMS on S-NPP and AMSR2 on GCOM-W1. The 51 levels were based on the previous 44 levels with additional levels added at the top of the profile (between 0.1 hPa and 10 hPa) to improve the representation of the stratosphere. However, this introduced a discrepancy in level spacing at the top of the atmosphere (Figure 1a).

For RTTOV-11, the new coefficient files are all based on a fixed set of 54 vertical pressure levels, derived from the following formula (Strow *et al.*, 2003):

$$p_{lev}(i) = (Ai^2 + Bi + C)^8 \quad (1)$$

where i is the level number. The constants A, B and C are determined by setting $p_{lev}(1)=1050$ hPa, $p_{lev}(33)=300$ hPa and $p_{lev}(54)=0.005$ hPa.

Figure 1b) shows the layer depth as a function of height for the 44, 51 and 54 versions of the RTTOV fixed pressure levels along with the 137 vertical levels of the current IFS atmospheric model. Compared with the current 44 or 51 RTTOV fixed pressure levels, the 54 RTTOV fixed pressure levels has additional stratospheric levels, more uniform varying layer thicknesses and enhanced resolution throughout the atmosphere.

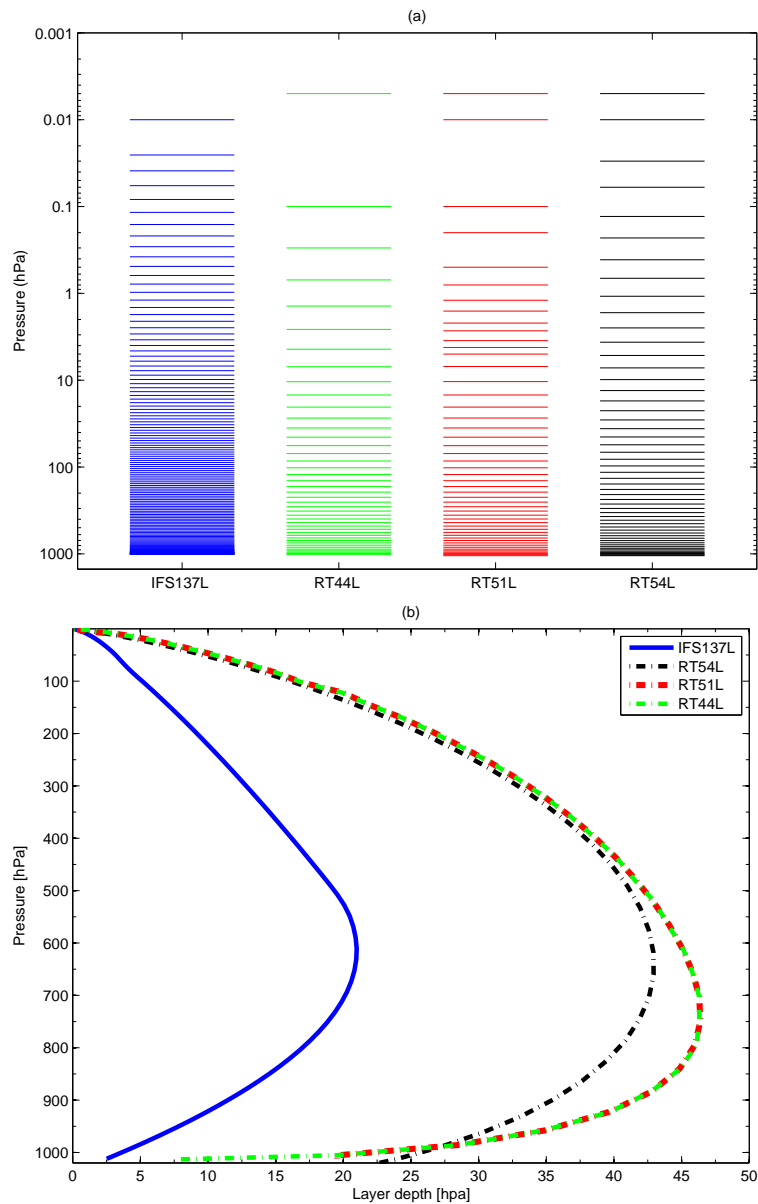


Figure 1: a) 137 vertical levels of the current IFS atmospheric model for a standard surface pressure (IFS137L, blue) along with the 44 (RT44L, green), 51 (RT51L, red) and 54 (RT54L, black) versions of the RTTOV fixed pressure levels; b) Layer depth as a function of height (both in hPa) for IFS137L (blue), RT44L (green), RT51L (red) and RT54L (black). The y-axis is logarithmic in (a) and linear in (b).

2.2 Line-by-line models and training atmospheric profiles sets

Characteristics of RTTOV-11 MW coefficient files are shown in Table 1. The AMSUTRAN line-by-line model, which is a version of the Liebe Millimeter-wave Propagation Model (MPM) developed over several versions over the last decade or so, is used to calculate channel-averaged transmittances to space, with water vapor (H_2O) as the only variable gas, and with oxygen (O_2), nitrogen (N_2) and, optionally, ozone (O_3) as mixed gases (Saunders *et al.*, 2012). The computation of the gaseous absorption is performed with the 1989 version of the Liebe MPM model (MPM89) for water vapor (Liebe, 1989), the 1993 version of the Liebe MPM model with coefficients from the Liebe MPM-92 model for mixed gases (Liebe *et al.*, 1993, 1992), and an adaptation of Liebe MPM-93 using High Resolution Transmission (HITRAN) line parameters for ozone (Rothman *et al.*, 2009). Ozone is only included for 183 GHz channels (Saunders *et al.*, 2012). The half-width of the 22 GHz water vapor line has been reduced in the MPM model to the more recent value given by the HITRAN molecular line database (Liljegren *et al.*, 2005). Instrument resolution transmittance spectra were computed for each atmospheric profile and six different zenith angles, namely, the angle for which the secant has equally spaced values from 1 to 2.25. The channel-averaged transmittances to space were calculated with a training dataset of 83 profiles (Matricardi, 2008) selected from the work of Chevallier *et al.* (2006) and interpolated to 101 levels. The horizontal resolution of the ECMWF forecast model used for the 83 profile set is about 25 km and the vertical levels are 91 with the top level at 0.01 hPa. The 83 profile training set has been considered representative of the range of variations in temperature and absorber amount found in the real atmospheres and has been used for all RTTOV-11 coefficient files generation. The coefficient file also defines which set of optical depth predictors to use. We use the so called predictors version 7, which has 10 predictors for mixed gases, 15 for water vapor and 11 for ozone (Saunders *et al.*, 1999).

Table 1: The LBL models and training atmospheric profiles sets in the new MW coefficient files.

MW Line by line model	Sensors
Liebe MPM	AMSU-A, TMI, SSMI, WINDSAT
Gases fixed= $O_2 + N_2$	AMSRE, AMSR2, MWRI, MWTS, MSU
Gases variable= H_2O	
Training set: 83 ECMWF profiles set	
Liebe MPM	SSMIS, MWHS, HSB
Gases fixed= $O_2 + N_2 + O_3$	GMI, MHS, ATMS
Gases variable= H_2O	
Training set: 83 ECMWF profiles set	

Concerning the old MW coefficient files used at ECMWF, the channel-averaged transmittances to space were calculated on various profile sets (Table 2): the 43 profiles set for a number of instruments including AMSU-A, SSMIS and TMI, the 52 profiles set picked from the 60 level ECMWF model for MHS and WINDSAT and the 83 profile set picked from the 91 level ECMWF model with ozone analysed variable for recent MW instruments as ATMS and AMSR2.

Table 2: The LBL models and training atmospheric profiles sets in the current MW coefficient files.

MW Line by line model	Sensors
Liebe MPM	
Gases fixed= $O_2 + N_2$	
Gases variable= H_2O	
Training set: TIGR-43 profiles set	AMSU-A, SSMI, SSMIS, TMI, AMSRE, MWTS, MWHS, MWRI, HSB, MSU
Training set: 52 ECMWF profiles set	WINDSAT
Training set: 83 ECMWF profiles set	AMSR2
Liebe MPM	
Gases fixed= $O_2 + N_2 + O_3$	
Gases variable= H_2O	
Training set: 52 ECMWF profiles set	MHS
Training set: 83 ECMWF profiles set	ATMS, GMI

To summarise, the most significant differences between the RTTOV-11 and the current MW regression coefficient files are:

- RTTOV-11 MW coefficients are provided on 54 fixed vertical pressure levels with additional stratospheric levels and smoothly varying layer thicknesses.
- RTTOV-11 coefficients are calculated with a training dataset of 83 ECMWF profiles, originally on 91 levels but interpolated to 101 levels.
- Ozone is included as mixed gas for sensors which have channels around 183 GHz (e.g., SSMIS, MWHS and HSB).
- A new value for the air-broadened half-width of the 22 GHz water vapor line is used for sensors like SSMIS (Liljegren *et al.*, 2005). AMSUTRAN uses a smaller half-width from the HITRAN molecular line database (a relative change of 5.5 %).

2.3 ECMWF-specific γ -corections on AMSU-A coefficients

AMSU-A observations on some of the platforms are corrected at ECMWF by scaling the optical depth in each layer by a constant γ before computing the layer transmission (Watts and McNally, 2004). The γ -correction values used operationally at ECMWF operations are shown in Table 3: they were derived empirically based on departure statistics from NWP and are of the order of a few percent on NOAA-15, -16, -18 and Aqua, while on MetOp-A, MetOp-B and NOAA-19, the AMSU-A instrument does not have such a correction applied ($\gamma = 1$). Attempts were made to update the γ -values and to harmonise the treatment of AMSU-A radiance data over the different platforms, but were not fully successful for an operational change (Di Tomaso and Bormann, 2010). We will revisit this in further work, also examining the possibility of accounting for shifts in the passband center frequencies for AMSU-A channels to improve the bias correction of AMSU-A data relative to NWP models (Lu and Bell, 2014). For now, the newly released AMSU-A coefficient files were updated off-line to use the same γ -correction values in channels 5-8 as used with the current AMSU-A coefficient files.

Table 3: Values of γ used in ECMWF operations.

Satellites Channel	NOAA-15	NOAA-16	NOAA-18	Aqua	MetOp-A/B NOAA-19
5	1.050	1.053	1.042	1.050	1.000
6	1.050	1.040	1.018	1.039	1.000
7	1.034	1.047	1.039	1.045	1.000
8	1.040	1.055	1.035	1.046	1.000

3 Evaluation of MW coefficient files on 54 levels in the IFS

3.1 Experiments set-up

To characterise the impact of the newly released NWP-SAF regression coefficient files for MW instruments, a set of two assimilation experiments covering a 8 month period (July 2013 to February 2014) was run with ECMWF's 12-h 4D-Var system model cycle 40r2 of the IFS, but with the satellite assimilation configuration for 40r3 to include:

- The all-sky assimilation of SSMIS on F-17 and four MHS sensors over ocean, land and sea-ice (Geer, 2013; Geer *et al.*, 2014).
- The assimilation of surface-sensitive ATMS humidity (channels 18-22) and temperature sounding (channels 6-8) over land (Lawrence and Bormann, 2014).
- Revised Kalman Filter atlas to apply a more physically based emissivity parametrisations (Bormann, 2014).
- Assimilation of GPS-RO with two-dimensional observation operator (Healy *et al.*, 2007).
- New options for vertical interpolation and Jacobian smoothing (Lupu and Geer, 2015).

The experiments have been run at reduced T511 horizontal resolution (40 km) and 137 vertical levels with the model top level pressure at 0.01 hPa and ten-day forecasts have been run from both the 00 UTC and 12 UTC analysis. A month's spinup has been excluded from the beginning of each experiment in order to allow the variational bias correction to adjust to the new bias resulting from the changes in the radiative transfer model. Both experiments assimilated the full ECMWF operational observing system of conventional and satellite observations. The conventional observation network consists of near-surface observations (land stations, ships and buoys) and upper-air data (radiosondes, dropsondes, aircraft, wind profilers and PILOTs). CRIS (S-NPP), MWHS (FY-3A, -3B) and MWTS (FY-3A) radiances were only passively monitored, while the set of assimilated satellite observations consisted of:

- MW Sounder radiances: AMSU-A (NOAA-15, -16, -18, -19, EUMETSAT's MetOp-A and MetOp-B platforms and NASA's Aqua platform), MHS (NOAA-18, -19, MetOp-A, MetOp-B) and ATMS (S-NPP);
- MW Imager radiances: SSMIS (F-17), TMI (TRMM);

- IR Sounder radiances: HIRS (MetOp-A, -B) and advanced sounder data from IASI (MetOp-A) and AIRS (Aqua);
- IR Imager radiances: CSR from geostationary satellites (GOES-East/West, Meteosat-7, MTSAT-2) and ASR (Meteosat-10);
- AMVs from geostationary satellites (GOES-East/West, Meteosat-7/10, MTSAT-2) and polar orbiting satellites MODIS(Aqua), AVHRR AMVs (NOAA-15,-16, -18, -19);
- A constellation of global positioning system radio occultation (GPSRO) sensors from GRAS (MetOp-A), COSMIC 1-6 and GRACE-A;
- Scatterometer wind vectors from ASCAT (MetOp-A, -B) and OceanSat-2 Scatterometer;
- Total column ozone products: SBUV instruments on NOAA-19 and OMI (Aura);

The experiments are summarised below:

- **CTRL:** Control ECMWF data assimilation and forecasting model with the full observing system and using the current IR and MW coefficient files from IFS.
- **Revised-MW:** Same system configuration, except that MW coefficient files have been replaced by the new RTTOV-11 files.

In both experiments a variational bias correction (VarBC) (Dee, 2005; Auligné *et al.*, 2007) is applied to the majority of satellite radiance data and to selected conventional observations with the aim of removing systematic error differences between simulations and observations that result from a combination of instrument, observation operator and forecast model biases. The bias parameters are fully integrated into the 4D-Var control variable and updated inside the NWP assimilation system. Changes in the radiative transfer will lead to different first guess departures which will lead to differences in the analyses or to differences in the bias correction.

3.2 Bias characteristics and departure statistics

One of the main changes in the MW coefficient file upgrade is the new specification of the 22 GHz water vapor line width and inclusion of ozone for channels near 183 GHz for sensors such as SSMIS. This leads to a reduction in the mean bias corrections, particularly in channels 12-13 (19 GHz) and 14 (22 GHz) compared to the bias corrections necessary with the current radiative transfer coefficients (Figure 2). This reflects better agreement with the observations before bias correction and lower forward model error as result of using improved spectroscopy. The humidity SSMIS sounding channels 9-10 (183 GHz) now have bias corrections of slightly larger magnitude. After bias correction, the changes in the mean biases of the first-guess (FG) are negligible, suggesting that the variational bias correction is successful in removing the biases in both experiments.

The AMSU-A observations are assimilated over land and sea surfaces but only in conditions diagnosed as clear and including a γ -adjustment in the radiative transfer calculations. Except for AMSU-A sensors on MetOp-B and NOAA-18, every AMSU-A has at least one broken channel as follows: channel 7 on MetOp-A, channels 6, 11 and 14 on NOAA-15, channels 8 and 9 on NOAA-16, channels 7 and 8 on

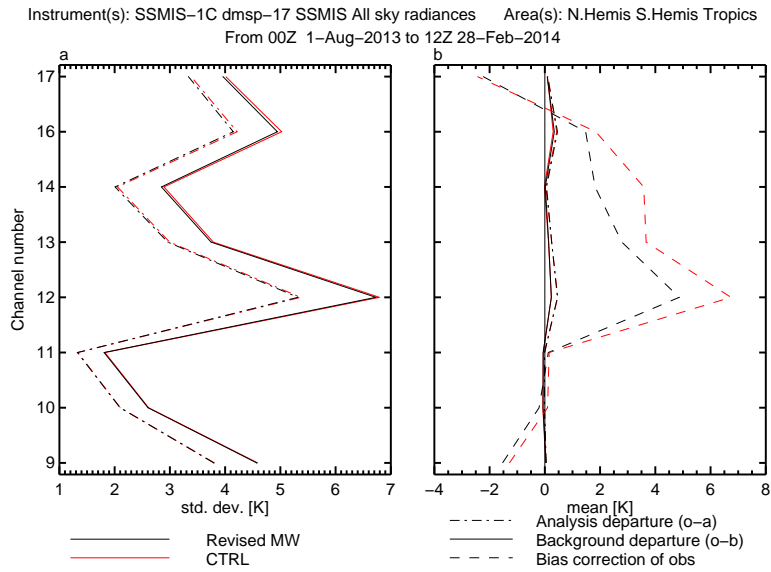


Figure 2: Standard deviations [K] (left panel) and means [K] (right panel) for FG departures (solid lines), analysis departures (dotted lines), and bias corrections (dashed lines) for used SSMIS radiances over the globe for the period 1 August 2013 - 28 February 2014 (observations minus FG or analysis, respectively). Statistics for the Revised-MW experiment are shown in black, whereas statistics for the CTRL experiment are shown in red.

NOAA-19 and channels 6 and 7 on Aqua. AMSU-A channel 14 is used to anchor the upper stratospheric temperature analysis within VarBC and is assimilated without a bias correction. All other channels are corrected for a global offset bias, a bias that varies depending on the location or air-mass, and a bias that varies depending on the instrument scan position.

Figure 3 and 4 shows maps of the FG-departures before and after the bias correction for AMSU-A channel 8 peaking at 150 hPa on Metop-A and NOAA-18 respectively, in the Revised-MW experiment for the very first 12-h assimilation cycle centered at 00 UTC 1 July 2013. When no γ -correction is applied as for the Metop-A satellite, the variational bias correction is effective in eliminating most of the air-mass-dependent errors. Moreover, when a γ -correction is applied as for the NOAA-18 satellite, the variational bias correction has to do less work as air-mass-dependent biases are significantly removed in the radiative transfer calculations.

For AMSU-A, considering the new RTTOV-11 coefficient files with more vertical levels and based on a more recent training set, a reduction of the absolute bias corrections is noticed for channels 10-13 (Fig. 5). Similar reductions in the absolute bias corrections are noticeable for the stratospheric channels 12-14 of the ATMS, presumably resulting from the use of more vertical levels in the RTTOV-11 coefficient file (not shown). Radiosonde temperature observations also show improvement in the bias against the first-guess and analysis between 10 and 70 hPa (Fig. 6).

The normalised standard deviation of the FG departure statistics for SSMIS, ATMS and AMSU-A after the bias correction are analysed through Figure 7. The results show improved FG fit for SSMIS channels globally. Significant improvements of up to 1.5% are found for SSMIS channel 14, in the 22 GHz water vapor line with vertical polarisation. For the 183 GHz SSMIS water vapor channels 9-11, the improvements of the FG fit are smaller, but significant (0.4 to 0.7%). These results reflect the improvements in the spectroscopy based on the narrowed 22 GHz line width and the addition of ozone absorption at 183 GHz.

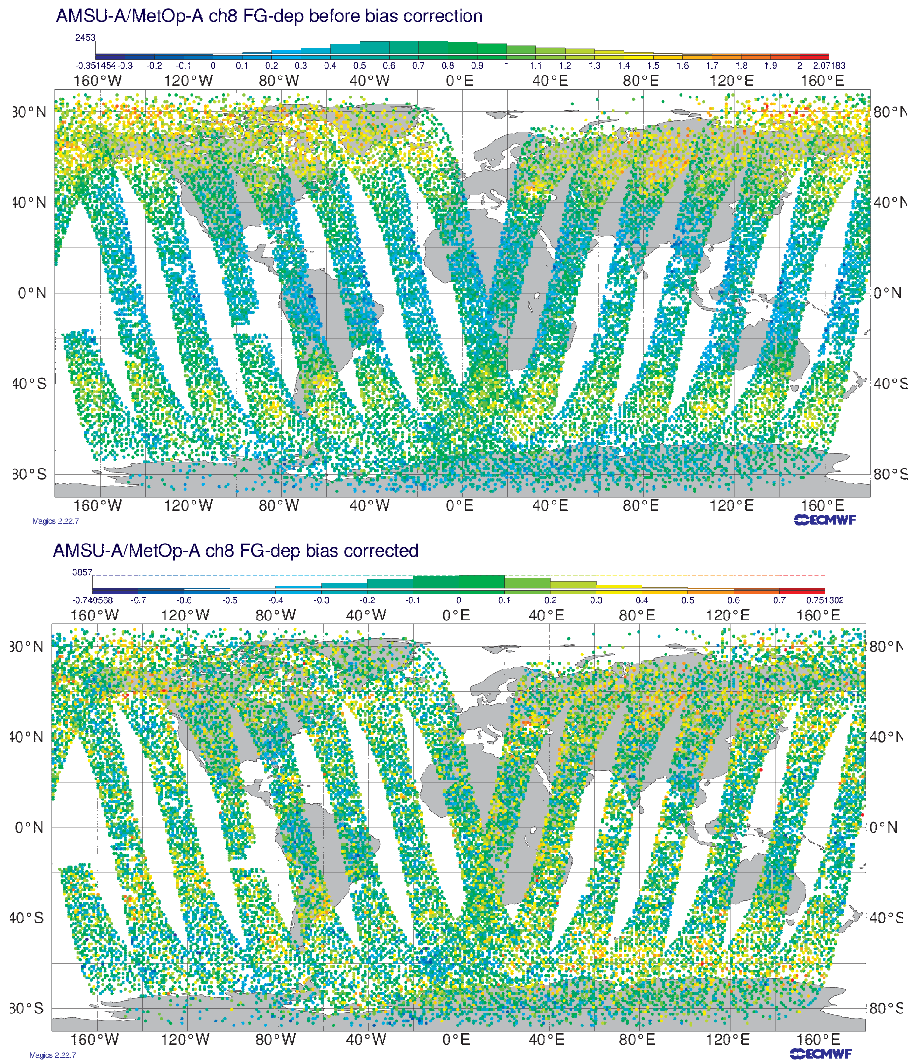


Figure 3: First-guess departure fields for assimilated AMSU-A observations in channel 8 onboard MetOp-A in Revised-MW experiment for the 12-h assimilation cycle centered at 00 UTC 1 July 2013: (a) before and (b) after variational bias correction.

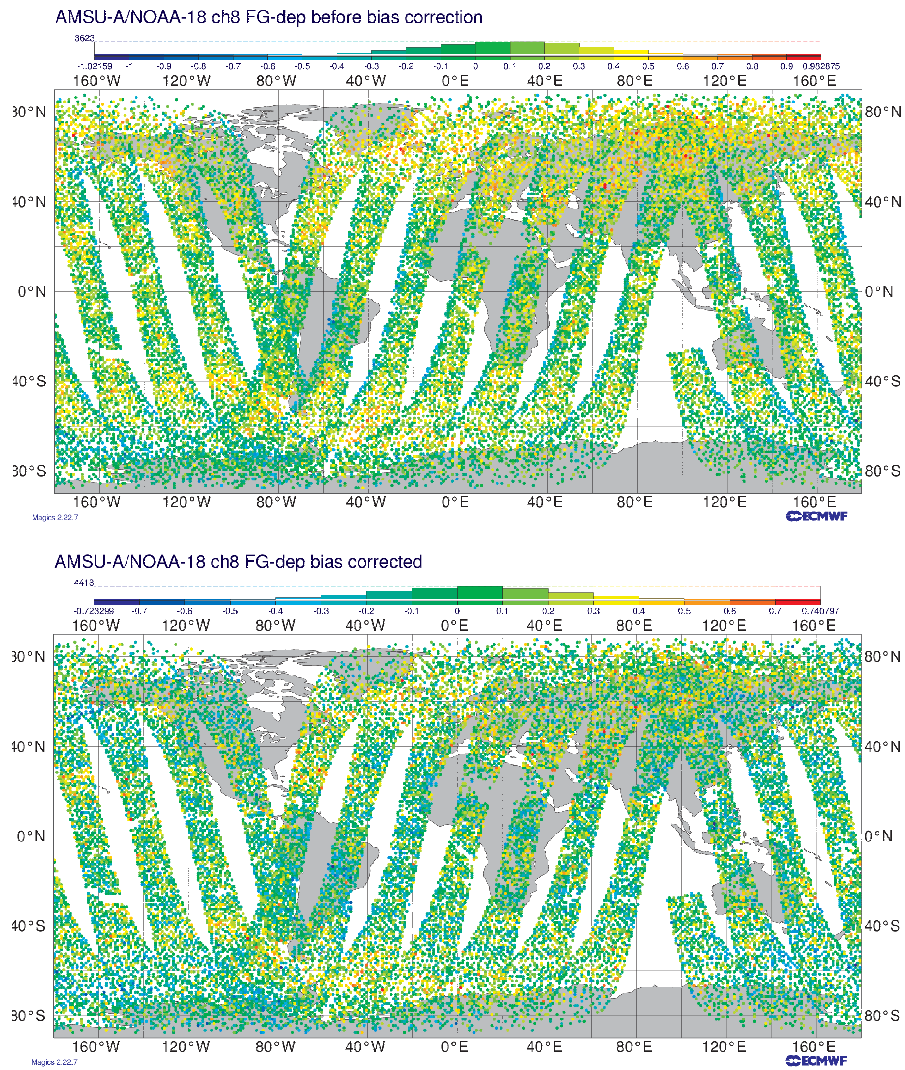


Figure 4: As Fig. 3, but for AMSU-A channel 8 onboard NOAA-18.

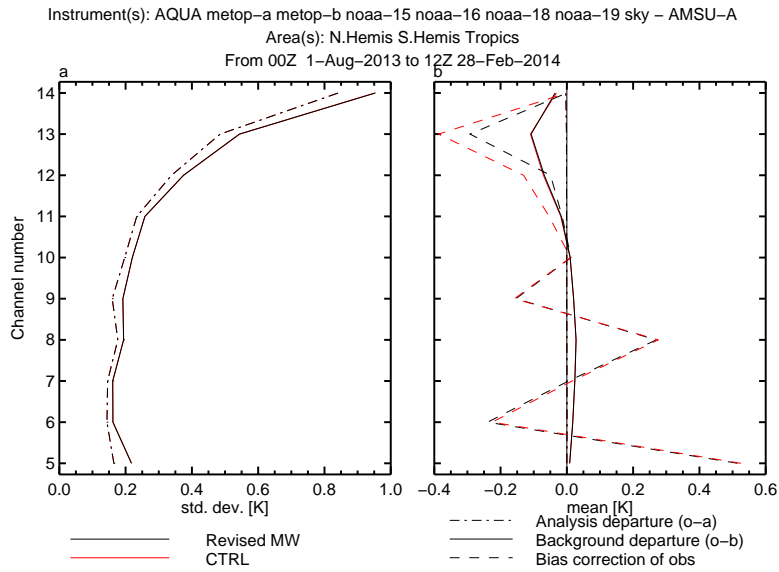


Figure 5: As Fig. 2 but for AMSU-A observations combined across all seven satellites: NOAA-15, -16, -18, -19, MetOp-A, MetOp-B and Aqua.

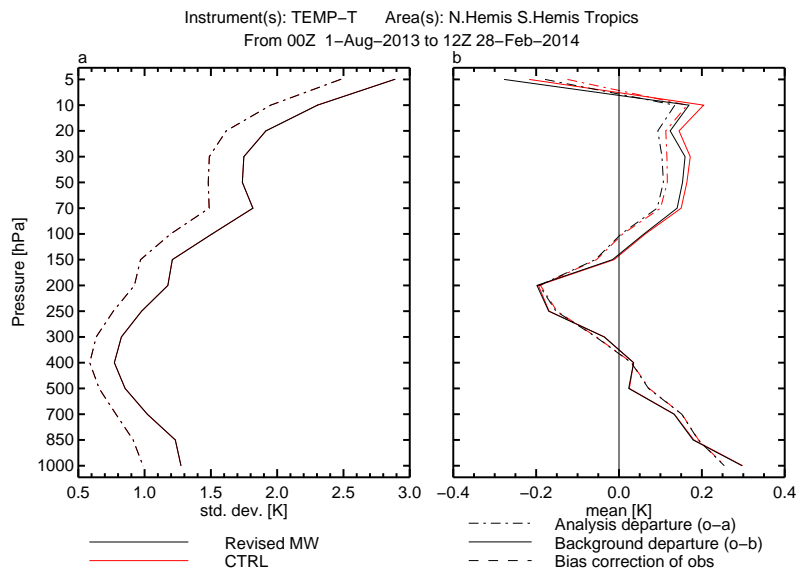


Figure 6: As Fig. 2 but for TEMP-T radiosonde observations.

A positive impact on humidity is also seen from ATMS channels 18-19, where improvements of up to 0.1% are noticeable. From the assimilation of ATMS temperature-sounding channels, reduced standard deviations of FG departures reaching 0.2% are seen in channels 12-13, having the weighting functions peaking at around 20 hPa and 10 hPa, respectively. Standard deviations of FG departures are also reduced for the AMSU-A channels 12-13, which measure the stratospheric temperature at 10 hPa and 5 hPa, respectively. This is most likely the result of the increased number of vertical layers used with the new coefficient files. At the same time, standard deviations of FG departures for ATMS channel 10 (peaking at around 80 hPa) and for AMSU-A channels 7-10 (peaking in the upper troposphere and lower stratosphere, 250-10 hPa) are increased. These slightly increased standard deviations are not considered a major problem: they are less evident in more recent testing (Section 4) and are counterbalanced by improvements in other FG fits to microwave instruments.

The FG fits to other observations (infrared radiances from instruments such as HIRS, IASI and AIRS, GPS, AMVs, aircraft temperature observations, specific humidity from radiosondes and in situ winds) are mostly similar between the Revised-MW and the Control experiments and the changes in the standard deviations of FG departures are not statistically significant.

Overall, the experiment using the new released MW coefficient files brings a statistically significant improvement in standard deviation of the FG departure statistics in the stratosphere and indicates small changes to the quality of the analyses. One other noteworthy difference is a small change in terms of differences in the mean analyses, notably some temperature changes of a few tenths of a degree over the polar regions in the stratosphere (Fig. 8). As this is above the level of radiosondes or most other verification data, it is hard to verify whether this is a true improvement or not, but at around 0.2 K this change is likely much smaller than the precision of any observations type available in the upper stratosphere.

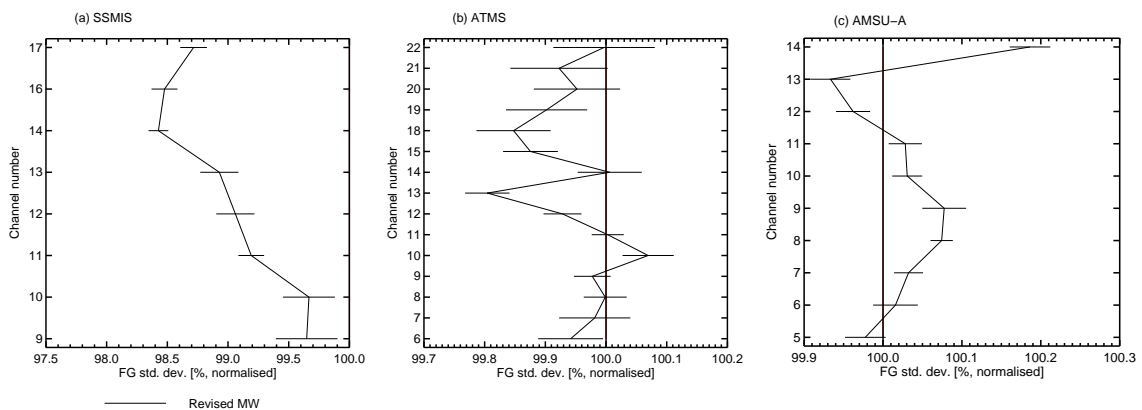


Figure 7: Normalised standard deviation of first-guess departures as a percentage relative to the control for: a) SSMIS on F-17 observations; b) ATMS on S-NPP observations; c) AMSU-A observations combined across all seven satellites. The area is global and the period is from 1 August 2013 to 28 February 2014. Error bars indicate the 95% confidence interval. Numbers less than 100% indicate beneficial impact.

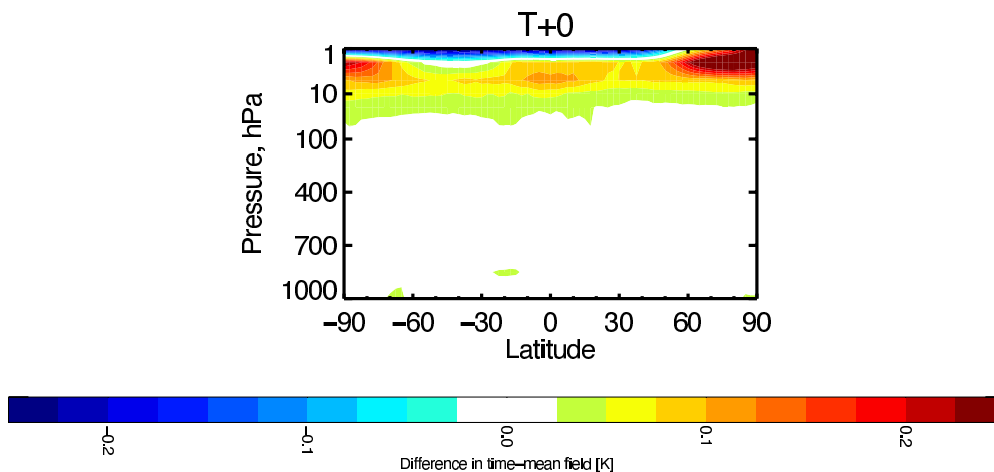


Figure 8: Difference in the zonal mean temperature analysis [K] between the Revised-MW experiment and the Control. The positive values, displayed in red colors, indicate warmer values in the Revised-MW experiment.

3.3 Impact on forecasts

Figure 9 shows the normalised difference in geopotential root-mean-square (RMS) errors at 500 hPa as function of the forecast time in both southern and northern extratropics. When verified against own-analyses, the forecast impact of RTTOV-11 with new MW coefficient files on headline scores is overall neutral.

Figures 10 and 11 show zonal mean plots of forecast error differences (Revised MW-CTRL) for temperature and vector wind for various forecast times (from T+12-h to T+72-h). Using the new MW coefficient files results in an improvement in statistical forecast scores of temperature (Figure 10) and relative humidity (not shown) in the upper stratosphere between 1-10 hPa. A mostly neutral impact is obtained in the forecast of the wind fields (Figure 11). The temperature scores at 2-5 hPa reflect better agreement between analysed mean temperature and forecast mean temperature, thanks to the small increase in analysed temperature (Fig. 8).

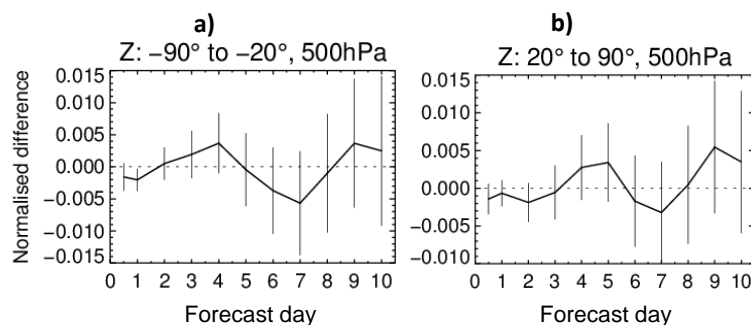


Figure 9: Normalized change in RMS forecast error in geopotential height at 500 hPa for: a) the southern extratropics; b) the northern extratropics. Negative values indicate a reduction in forecast error and hence a beneficial impact on forecasts. Verification is against own analysis and scores are based on 404 to 423 forecasts on a seven month period, August 2013 to February 2014. Error bars give the 95% confidence limits.

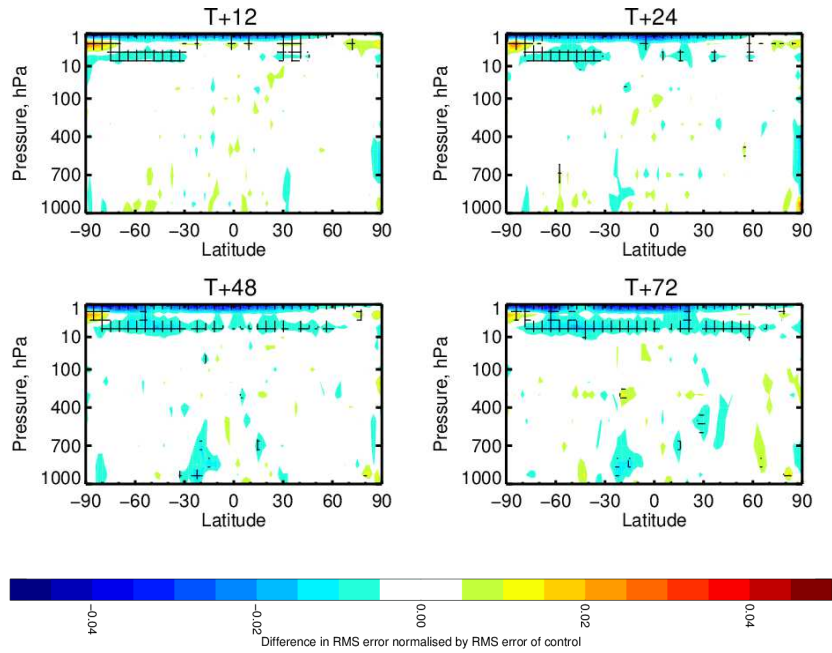


Figure 10: Normalised change in the RMS of temperature forecast error. Verification is against own analysis and scores are based on the combined 7 months of experimentation, August 2013 to February 2014. Cross-hatched areas show changes that are significant at the 95% confidence level. Negative values (blue colors) indicate a reduction in RMS error and show an improvement compared to the control.

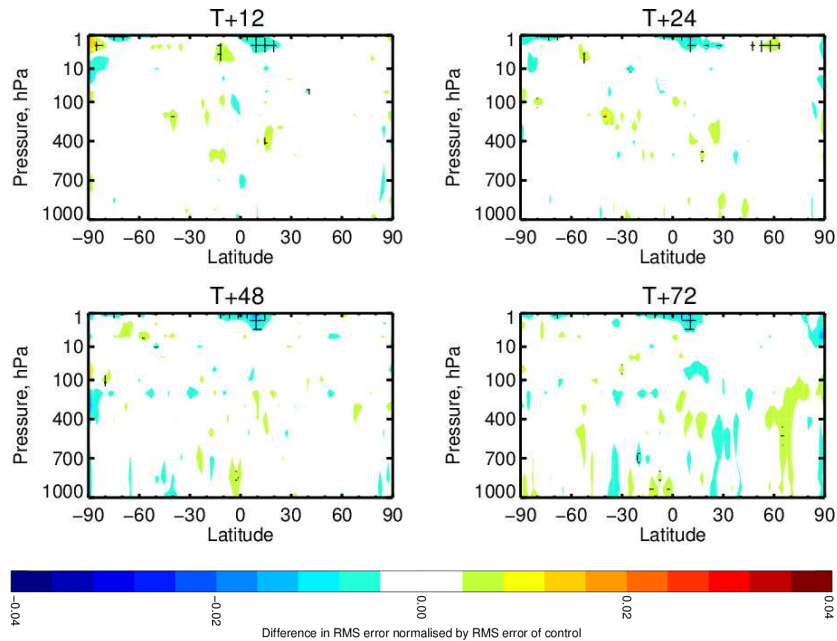


Figure 11: Same as Figure 10 but for vector wind.

4 Impact assessment of the MW coefficients upgrade for operational implementation

A second set of Control and Revised-MW experiments were run over a combined six months winter and summer period (February to April 2014 and June to September 2014) in research mode using the cycle 41r1 version of the ECMWF analysis and forecasting system. This model cycle includes several changes to model physics, assimilation, observation usage and the ensemble configuration and is planned to become operational at ECMWF in May 2015.

With respect to the previous set of experiments, the new set of experiments were run with a horizontal truncation of T639 (which roughly corresponds to a horizontal resolution of about 32 km) over the standard 137 vertical levels that span the atmosphere from the surface up to 0.01 hPa. The new set of Control and Revised-MW experiment used all observations that were assimilated in ECMWF operations at the time of this study. Changes in the observation usage with respect to experiments described in Section 3 include: IASI and GRAS on MetOp-B are now assimilated, AMSR-2 on GCOM-W1 is passively monitored, while AMSU-A on NOAA-16, MWTS and MWHS on FY-3A, OceanSat-2 Scatterometer and GRACE-A are no longer available as these instruments failed.

In the following we summarise the main results of using the RTTOV-11 coefficient files in the IFS. The modifications to the observation departure statistics are consistent with results described in Section 3, that is, improvement in the standard deviations of FG departures for SSMIS channels, with the most significantly improved channel being the one in the 22 GHz water vapor line (channel 14) and for ATMS and AMSU-A stratospheric channels (Figure 12). A small increase of up to 0.1% is noticed for standard deviation of FG departure for AMSU-A channel 8 in Revised-MW experiment. Departure statistics for other observations are not significantly altered compared to the Control (Figure 13). Small changes to the mean analyses are noticed above 100 hPa, with changes to the mean analysis of temperature less than 0.2 K (Figure 14).

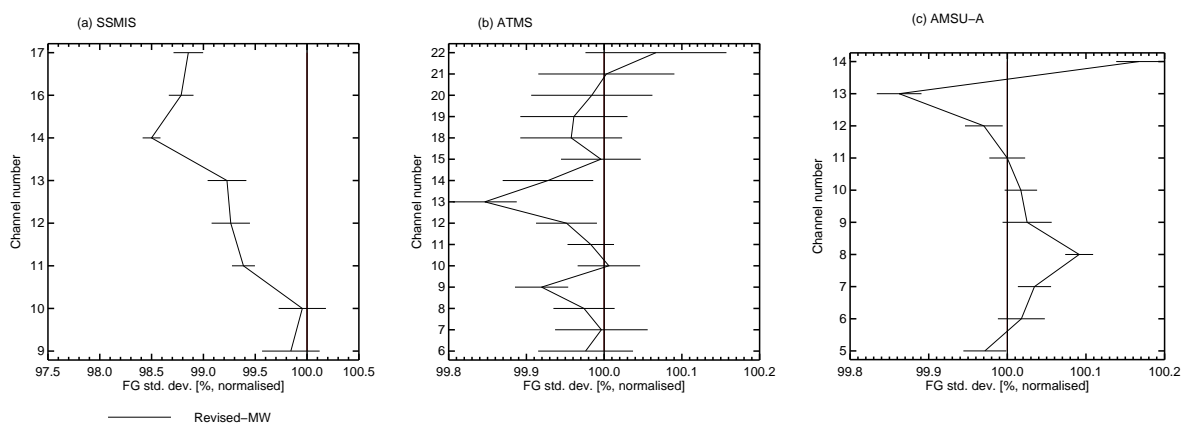


Figure 12: Normalised standard deviation of first-guess departures as a percentage relative to the control for: a) SSMIS on F-17 observations; b) ATMS on S-NPP observations; c) AMSU-A observations combined across all six satellites: NOAA-15, -18, -19, MetOp-A, MetOp-B and Aqua. The area is global and the period combine results from summer and winter experiments covering six months in 2014. Error bars indicate the 95% confidence interval. Numbers less than 100% indicate beneficial impact.

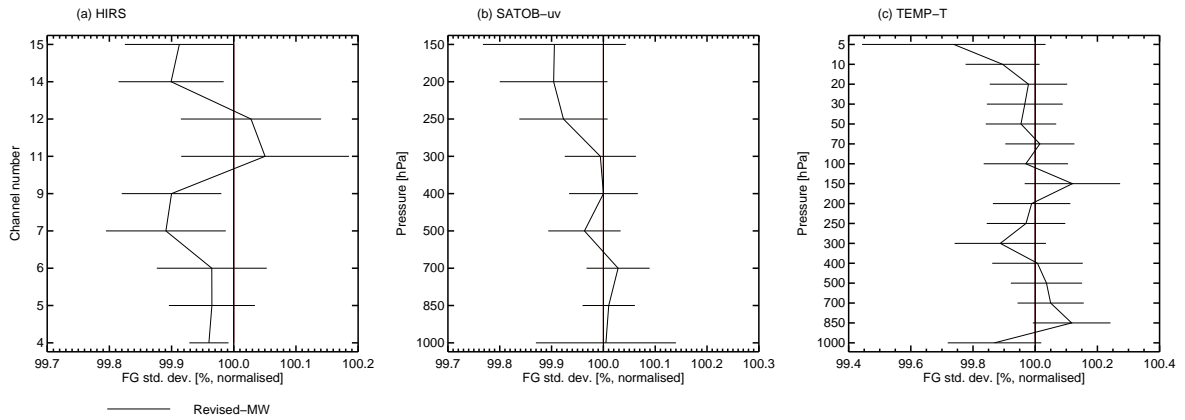


Figure 13: As Fig. 12 but for: a) HIRS observations; b) Atmospheric Motion Vectors combining statistics from u and v-wind components; c) TEMP-T radiosondes observations.

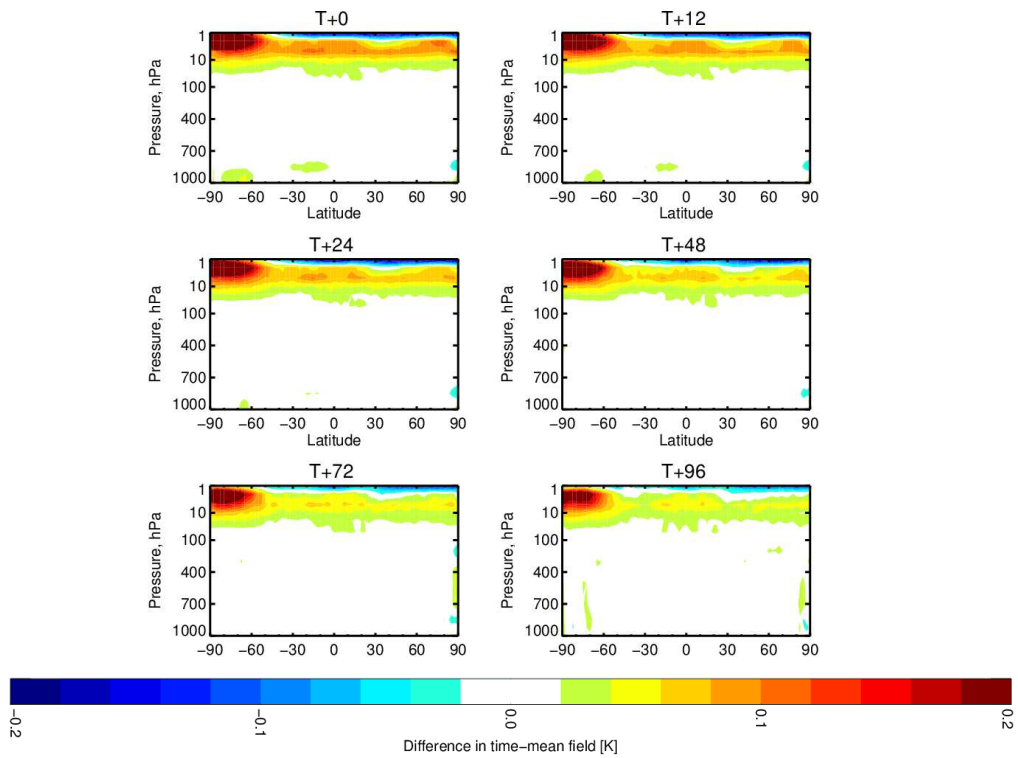


Figure 14: Difference in the zonal mean temperature analysis and forecasts [K] between the Revised-MW experiment and the Control. The period combines results from summer and winter experiments covering six months in 2014. The positive values, displayed in red colors, indicate warmer values in the Revised-MW experiment.

For forecast scores, the summer and winter runs have been combined to give about 6 months of verification. The impact on headline forecast scores was fairly neutral overall (not shown). The normalised changes in RMS errors in temperature are shown in Figure 15 as a function of latitude and pressure for various forecast times from T+12-h to T+120-h. In general, there is a decrease in RMS temperature errors between 1-10 hPa from 12-h to 120-h. As mentioned before, this is related to a systematic change in the mean analysed temperature (warming of around 0.2 K) as shown in Figure 14.

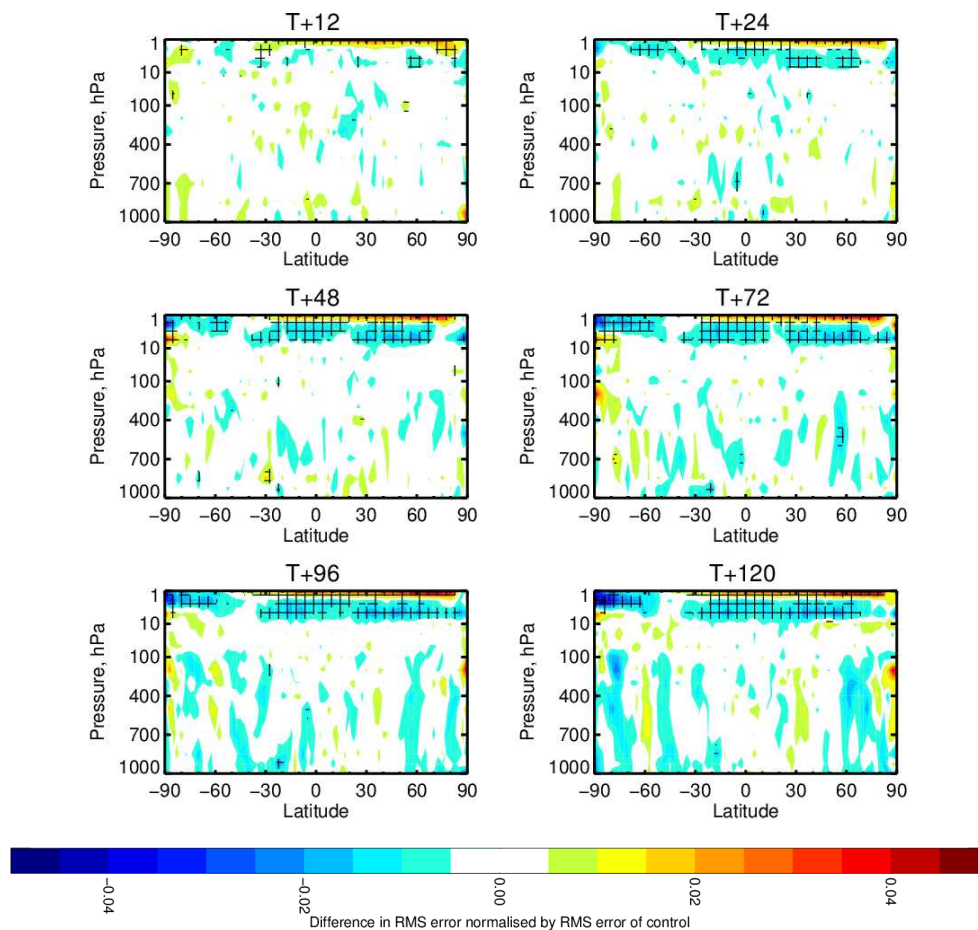


Figure 15: Normalised change in the RMS of temperature forecast error. Verification is against own analysis and scores are based on the combined 6 months of experimentation, February 2014 to April 2014. Cross-hatched areas show changes that are significant at the 95% confidence level.

5 Summary and Outlook

A new set of radiative transfer coefficients describing the regressions for the layer optical depths as a linear combination of profile dependent RTTOV version 7 predictors has been released with RTOV-11 for various infrared and microwave sounders and imagers. This report investigated the possibility of using with RTTOV-11 the new set of MW coefficient files, and summarises their impact on analyses and forecasts in the ECMWF system.

The upgrade included a revised line width parameter in the spectral region around the 22 GHz water vapor absorption. This has been used to generate new line-by-line simulations which have in turn been used to generate new SSMIS coefficients. Extensive experimentation conducted with the IFS cycles 40r2 and 41r1 shows that incorporating this new line width parameter significantly improves the FG fit for SSMIS imager channel 14 globally. Smaller but significant improvements of the FG fit are also found for SSMIS channels being centered on the 183 GHz water vapor.

After bias correction, FG departure statistics for most assimilated radiances are overall largely unaltered. However, we found reductions in the size of FG departures for ATMS and AMSU-A stratospheric channels resulting from the RTTOV-11 coefficients with more vertical levels on which the optical depth calculation is performed. The change to 54 levels ensure smooth varying layer thicknesses in particular at the top of the atmosphere and smooth Jacobians. This also leads to small differences in the mean temperature analysis especially above 100 hPa.

The results presented here suggested that it would be beneficial for the ECMWF operational system to use the most up-to-date version of the MW coefficient files released with the latest version of RTTOV-11. The forecast impact on headline scores over the two periods considered is overall neutral. Given the overall improvement in terms of first-guess fits for the microwave instruments and otherwise neutral forecast performance, the upgrade of the MW coefficient files has been included in cycle 41r2 of the IFS.

Based on work by [Lu and Bell \(2014\)](#), shifted coefficient files have been made available for AMSU-A instruments on several platforms to include new shifted channel center frequencies for the tropospheric sounding channels 6-8. Further evaluation is needed to evaluate their impact in the ECMWF analysis and forecast system and this will be reported in the future alongside another look at γ -corrections.

In the future, attention will also be given to the new IR regression coefficients files based on 54 levels and the improved line-by-line radiative transfer model LBLRTM v12.2. Their impact in the IFS will be assessed and compared against the current IR regression coefficients. It is expected that the new regression coefficients will improve the accuracy of the infrared radiance simulation.

Acknowledgements

Stephen English is gratefully thanked for reviewing the manuscript. The first author acknowledges the funding provided through the EUMETSAT NWP-SAF programme.

References

- Auligné, T., A. P. McNally and D. P. Dee, 2007: Adaptive bias correction for satellite data in a numerical weather prediction system. *Q. J. R. Meteorol. Soc.*, **133**, 631-642.
- Bormann, N., 2014: Reformulation of the emissivity Kalman Filter atlas, *ECMWF RD Memorandum*, RD14-190, ECMWF, Reading, UK.
- Cardinali, C., 2009: Monitoring the observation impact on the short-range forecasts. *Quart. J. Roy. Meteor. Soc.*, **135**, 239-250..
- Chevallier, F., S. Di Michele and A. P. McNally, 2006: Diverse profile datasets from the ECMWF 91-level short-range forecasts. *NWP-SAF Report*, NWPSAF-EC-TR-010.
- Clough, S.A, M. J. Iacono and J.-L. Moncet, 1992: Line by line calculation of atmospheric fluxes and cooling rates: application to water vapor. *J. Geophys. Res.*, **98**, 15761-15785.
- Dee, D., 2005: Bias and data assimilation. *Q. J. R. Meteorol. Soc.*, **131**, 3323-3343.
- Di Tomaso, E. and N. Bormann, 2010: Assimilation of ATOVS radiances at ECMWF: first year EU-METSAT fellowship report. *EUMETSAT/ECMWF Report*, **22**, ECMWF, Reading, UK.
- Geer, A. J., 2013: All-sky assimilation: better snow-scattering radiative transfer and addition of SSMIS humidity sounding channels. *ECMWF Tech. Memo.*, **706**, ECMWF, Reading, UK.
- Geer, A. J., F. Baordo, N. Bormann and S. English, 2014: All-sky assimilation of microwave humidity sounders, *ECMWF Tech. Memo.*, **741**, ECMWF, Reading, UK.
- Healy, S. B., J. R. Eyre, M. Hamrud and J.-N. Thépaut, J.-N., 2007: Assimilating GPS radio occultation measurements with two-dimensional bending angle observation operators. *Q.J.R. Meteorol. Soc.*, **133**: 1213-1227.
- Hocking, J., P. J. Rayer, D. Rundle, R. W. Saunders, M. Matricardi, A. Geer, P. Brunel and J. Vidot, 2014: RTTOV v11 Users Guide, *NWP-SAF report*, Met.Office, UK, 114pp.
- Hocking, J., 2014: Interpolation methods in the RTTOV radiative transfer model. *Forecasting Research Technical report*, **562**, Met Office, UK.
- Lawrence, H. and N. Bormann, 2014: First year report: The impact of HIRS on ECMWF forecasts, adding ATMS data over land and sea ice and new observation errors for AMSU-A. *EUMETSAT/ECMWF Report*, **34**, ECMWF, Reading, UK.
- Liebe, H., 1989: MPM - an atmospheric millimetre-wave propagation model. *Int. J. Infrared Milli.*, **10**, 631-650.
- Liebe, H., P. Rosenkranz and G. Hufford, 1992: Atmospheric 60-GHz oxygen spectrum: New laboratory measurements and line parameters. *J. Quant. Spectrosc. Radiat. Transfer*, **48**, 629-643.
- Liebe, H. and T. A. Dillon, 1969: Accurate foreign-gas broadening parameters of the 22-GHz H₂O line from refraction spectroscopy. *J. Chem. Phys.*, **50**, 727-732.
- Liebe, H., G. A. Hufford and M. G. Cotton, 1993: Propagation modeling of moist air and suspended water/ice particles at frequencies below 1000 GHz. Atmospheric propagation effects through natural and man-made obscurants for visible to mm-wave radiation, AGARD-CP-542, NATO, 3-13-11.

- Liljegren, J. C., S.-A. Boukabara, K. Cady-Pereira and S. A. Clough, 2005: The Effect of the Half-Width of the 22 GHz Water Vapor Line on Retrievals of Temperature and Water Vapor Profiles With a 12-Channel Radiometer, *IEEE Trans. Geosci. Remote Sens.*, **43**, 1102-1108.
- Lu, Q. and W. Bell, 2014: Characterizing Channel Center Frequencies in AMSU-A and MSU Microwave Sounding Instruments. *J. Atmos. Oceanic Technol.*, **31**, 1713-1732.
- Lupu C. and A. J. Geer, 2015: Evaluation and operational implementation of the RTTOV-11 in the IFS, *ECMWF Tech. Memo.*, **748**, ECMWF, Reading, UK.
- Matricardi, M., F. Chevallier, G. Kelly and J.-N. Thépaut, 2004: An improved general fast radiative transfer model for the assimilation of radiance observations. *Q. J. Roy. Meteorol. Soc.*, **130**, 153-173.
- Matricardi, M., 2008: The generation of RTTOV regression coefficients for IASI and AIRS using a new profile training set and a new line-by-line database. *ECMWF Tech. Memo.*, **564**, ECMWF, Reading, UK.
- Rothman, L. S., I. E. Gordon, A. Barbe, D. C. Benner, P. F. Bernath, M. Birk, V. Boudon, L. R. Brown, A. Campargue, J.-P. Champion, K. Chance, L. H. Coudert, V. Dana, V. M. Devi, S. Fally, J.-M. Flaud, R. R. Gamache, A. Goldman, D. Jacquemart, I. Kleiner, N. Lacome, W. J. Lafferty, J.-Y. Mandin, S. T. Massie, S. N. Mikhailenko, C. E. Miller, N. Moazzen-Ahmadi, O. V. Naumenko, A. V. Nikitin, J. Orphal, V. I. Perevalov, A. Perrin, A. Predoi-Cross, C. P. Rinsland, M. Rotger, M. Simeckova, M. A. H. Smith, K. Sung, S. A. Tashkun, J. Tennyson, R. A. Toth, A. C. Vandaele, J. Vander Auwera, 2009: The HITRAN 2008 molecular spectroscopic database. *J. Quantit. Spectrosc. Radiat. Transfer*, **110**, 533-572.
- Saunders, R., Matricardi, M. and Brunel, P., 1999: An improved fast radiative transfer model for assimilation of satellite radiance observations. *Q. J. R. Meteorol. Soc.*, **125**, 1407-1425.
- Saunders R., J. Hocking, P. Rayer, M. Matricardi, A. Geer, N. Bormann, P. Brunel, F. Karbou and F. Aires, 2012: RTTOV-10: Science and validation report. *NWP-SAF report*, Met.Office, UK, 31pp.
- Saunders R., J. Hocking, D. Rundle, P. Rayer, M. Matricardi, A. Geer, C. Lupu, P. Brunel, J. Vidot, 2013: RTTOV-11: Science and validation report. *NWP-SAF report*, Met.Office, UK, 62pp.
- Strow, L. L., S. E. Hannon, S. DeSouza-Machado, H. E. Motteler, and D. Tobin, 2003: An overview of the AIRS radiative transfer model. *IEEE Trans. Geosci. Remote Sens.*, **41**, 303-313.
- Watts, P. and A.P. McNally, 2004: Identification and correction of radiative transfer modelling errors for atmospheric sounders: AIRS and AMSU-A. In *Proceedings of the ECMWF Workshop on Assimilation of High Spectral Resolution Sounders in NWP*, ECMWF, Reading, UK.

APPENDIX I: Acronyms

ECMWF	European Centre for Medium Range Weather Forecast
EUMETSAT	European Organisation for the Exploitation of Meteorological Satellites
NASA	National Aeronautics and Space Administration
NOAA	National Oceanic and Atmospheric Administration

Instruments

AIRS	Atmospheric InfraRed Sounder
AMSR2	Advanced Microwave Scanning Radiometer 2
AMSU-A	Advanced Microwave Sounding Unit-A
ATMS	Advanced Technology Microwave Sounder
ASCAT	Advanced SCATterometer
AVHRR	Advanced Very High Resolution Radiometer
CRIS	Cross-track Infrared Sounder
GOES	Geostationary Operational Environmental Satellite
GPSRO	Global positioning system radio occultation
HIRS	High Resolution Infrared Radiation Sounder
HSB	Humidity Sounder for Brazil
IASI	Infrared Atmospheric Sounding Interferometer
MODIS	Moderate Resolution Imaging Spectroradiometer
MHS	Microwave Humidity Sounder
MWHS	MicroWave Humidity Sounder
MWTS	Microwave Temperature Sounder
MTSAT	Multi-functional Transport Satellite
OMI	Ozone Monitoring Instrument
SBUV	Solar Backscatter Ultraviolet Radiometer
SEVIRI	Spinning Enhanced Visible and Infrared Imager
SSMIS	Special Sensor Microwave Imager/Sounder
TMI	Tropical Rainfall Measuring Mission Microwave Imager

Satellites

COSMIC	Constellation Observing System for Meteorology, Ionosphere and Climate
DMSP-F17	Defense Meteorological Satellite F-17
FY-3A(B)	Feng-Yun-3A(B)
GCOM-W1	Global Change Observation Mission-Water1
GMI	Global Precipitation Measurement Microwave Imager
GRACE	Gravity Recovery and Climate Experiment
GRAS	GNSS (Global Navigation Satellite System) Receiver for Atmospheric Sounding
MetOp-A(B)	Meteorological Operational Satellite-A(B)
METEOSAT	European Geostationary Meteorological Satellite (EUMETSAT)
OceanSat-2	Satellite for the Ocean-2
S-NPP	Suomi National Polar-Orbiting Partnership
TRMM	Tropical Rainfall Measuring Mission

APPENDIX II: Abbreviations

4D-Var	Four-dimensional variational data assimilation
AMVs	Atmospheric Motion Vectors
ASR	All Sky Radiances
CSR	Clear Sky Radiances
FG	First Guess
HITRAN	HIgh-resolution TRANsmission molecular absorption database
IFS	Integrated Forecasting System
IR	Infrared
LBL	Line-by-Line
LBLRTM	Line-by-Line Radiative Transfer Model
MPM	Millimeter-wave Propagation Model
MW	Microwave
NWP	Numerical Weather Prediction
RTTOV	Radiative Transfer for the Television Infrared Observation Vertical Sounder
SAF	Satellite Application Facility
TIGR	Thermodynamic Initial Guess Retrieval
VarBC	Variational Bias Correction
WV	Water vapor